2008 IEEE International Conference on
Robotics and Automation
Pasadena, CA, USA, May 19-23, 2008

Control of 3-dimensional Snake Robots by Using Redundancy

Motoyasu Tanaka and Fumitoshi Matsuno

***Abstract*— In this paper, we consider the trajectory tracking control of a 3-dimensional (3D) snake robot by using redundancy. We discuss the motion control which accomplishes the trajectory tracking and other tasks, for example singular configuration avoidance, obstacle avoidance, etc., for the 3D snake robot. Features of the internal motion caused by the kinematic redundancy are considered and the dynamic model of the 3D snake robot is derived by introducing shape controllable points. By utilizing redundancy, we propose the controller which accomplishes the trajectory tracking as the main-task and several sub-tasks. Simulation results show the effectiveness of the proposed controller.**

I. INTRODUCTION

Unique and interesting gait of the snakes makes them able to crawl, climb a hill, climb a tree by winding and move on very slippery floor. It is useful to consider and understand the mechanism of the gait of the snakes for mechanical design and control law of snake robots. Hirose has long investigated snake robots and produced several snake robots, and he models the snake by a wheeled link mechanism (passive wheels are attached at the side of the snake robot body.) with no side slip [1]. A snake robot based on a wheeled link mechanism (wheeled snake robots) needs to avoid a singular configuration [2].

For 2-dimensional (2D) snake robots, we find that introduction of links without wheels and shape controllable points in the snake robot's body makes the system redundancy controllable based on the kinematic model [3]. We proposed the trajectory tracking controller based on the kinematic model [3] and based on the dynamic model [4]. Using the proposed control law and controlling shape controllable points, the robot can accomplish the trajectory tracking of the head position without converging to the singular configuration. The shape controllable point means the joint angles that we can control for adjusting the shape of the snake robot [4].

For 3-dimensional (3D) snake robots, Ma derived the model with considering Coulomb friction for the interaction with the environment and developed the simulator [5]. Date and Takita proposed a continuum model for the 3-dimensional snake-like creeping locomotion and the control method by discretizing the optimal bending moment [6]. However, in these studies there is no discussion about the trajectory tracking control of the snake-head. Based on the dynamic model, Yamakita proposed the controller using the constraint force of passive wheels but the sigularity avoidance does not ensure theoreticaly. There exists a trade-off between the singulality avoidance and the convergence of the tracking error [7]. We also proposed the trajectory tracking controller of 3D snake robots based on kinematic model [8].

This work was supported by JSPS Research Fellowships for Young Scientists.

M. Tanaka and F. Matsuno are with The University of Electro-Communications, Chofugaoka 1-5-1, Chofu, Tokyo, Japan {m-tanaka, matsuno}@hi.mce.uec.ac.jp

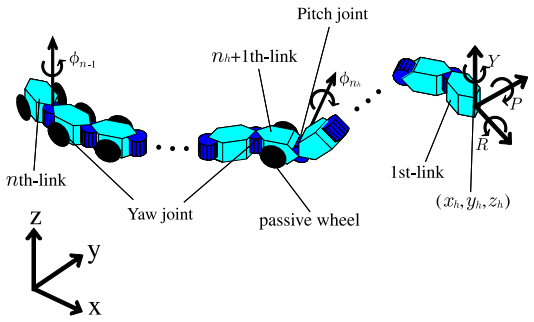

Fig. 1. An n-link 3D snake robot

A snake robot is similar to mobile manipulators [9] when some top links (the head part) of it are lifted up from the ground. In this case the head part of it can act as a hand of a manipulator. But a snake robot is essentially different from a mobile manipulator. Although a mobile manipulator has two separate mechanisms which accomplish locomotion and manipulation tasks independently, a snake robot has two functions, locomotion and manipulation, and it can change the functions adaptively. A snake robot can accomplish various complicated tasks by using redundancy, and an example task has been discussed in [10].

In this paper, we consider the trajectory tracking controller of a 3D snake robot based on the dynamic model. A pupular approach for control of a redundant manipulator is controlling internal dynamics related to the kinamtical redundancy by using the basis of the internal motion [11]. Same approach can be applied to the snake-like robot. In this approach deriving the basis and obtaining its differential are very difficult especially for the complicated nonlinear system such as snake robots. So we consider features of the internal motion caused by the kinematic redundancy and introduce the shape controllable point (SCP) [3][4] on the dynamic model of a 3D snake robot. By utilizing the kinematic redundancy, we propose the trajectory tracking controller which accomplishes several sub-tasks. Simulations have been carried out to demonstrate the effectiveness of the controller.

II. MODEL

We consider an n link wheeled 3D snake robot as shown in Fig. 1. All wheels are passive and all joints are active

and we assume that a passive wheel does not slide to the side direction. The length of the link is $2l$, the wheel is attached at the middle point of the link, and the distance between the middle of link and the center of wheel is l_w[m]. For simplicity, let us define that the head part is constructed from the first link to the n_h-th link, the base part is from the n_h+1 to the n-th link and the composition of the head and base part does not change. The number of links of the head part is n_h and that of the base part is n_b. We introduce following assumptions.

[Assumption 1] : Each joint rotates around the pitch or yaw axis.
[Assumption 2] : All joints of the base part rotate around the yaw axis, and the connected joint between the head and base part rotates around the pitch axis.
[Assumption 3] : Environment is flat.
[Assumption 4] : The robot is supported by the wheels of the base part and the head part is not contact with the ground.
[Assumption 5] : The n_h+1-th link (the top link of the base part) is wheeled.

By Assumption 1-4, all wheels of the base part contact environment and the head part can move without the constraint from the environment. Assumption 5 is introduced in order to separate the head part and the base part clearly.

The flat environment corresponds to the xy plane of the inertial coordinate system O-xyz. Let $\boldsymbol{w} = [x_h, y_h, z_h, R, P, Y]^T$ be the position and the attitude of the snake head with respect to O-xyz. Let $\boldsymbol{\phi}=[\phi_1, \cdots, \phi_{n-1}]^T$ be the set of relative joint angles, $\boldsymbol{\tau} = [\tau_1, \cdots, \tau_{n-1}]^T$ be the set of joint torques. Let us define $\boldsymbol{q} = [\boldsymbol{w}^T, \boldsymbol{\phi}^T]^T \in \mathbf{R}^{n+5}$. The position and the attitude of the snake head should be 6 DOF and the base joint of the head part can move on 2D plane since the movement of the base part is constrained on the xy plane. Thus the head part needs to have at least four joints or four links in order to accomplish an arbitrary position and attitude of the snake head. Kinematic redundancy occurs by increasing the number of the head links and its DOF m_h is $m_h = n_h - 4$.

In the case where all links of the base part are wheeled, the kinematic equation based on the velocity constraint by passive wheels is expressed as

$$A(\boldsymbol{q})\dot{\boldsymbol{w}} = B(\boldsymbol{q})\dot{\boldsymbol{\phi}} \tag{1}$$

where $A \in \mathbf{R}^{(n_b+3)\times 6}$, $B \in \mathbf{R}^{(n_b+3)\times(n-1)}$,

$$B = \begin{bmatrix} b_{11} & \cdots & b_{1n_h} & & & \mathbf{0} \\ b_{21} & \cdots & b_{2n_h} & -l & & \\ \vdots & & \vdots & & \ddots & \\ b_{n_b1} & \cdots & b_{n_bn_h} & b_{n_b(n_h+1)} & \cdots & -l \\ b_{(n_b+1)1} & \cdots & b_{(n_b+1)n_h} & 0 & \cdots & 0 \\ b_{(n_b+2)1} & \cdots & b_{(n_b+2)n_h} & 0 & \cdots & 0 \\ b_{(n_b+3)1} & \cdots & b_{(n_b+3)n_h} & 0 & \cdots & 0 \end{bmatrix}. \tag{2}$$

Considering the snake robot that m_b passive wheels corresponding to the $i_1, \cdots, i_{m_b}$-th links are removed and let us define $m = m_h + m_b$, the kinematic equation based on the velocity constraint by passive wheels is expressed as

$$\bar{A}(\boldsymbol{q})\dot{\boldsymbol{w}} = \bar{B}(\boldsymbol{q})\dot{\boldsymbol{\phi}}. \tag{3}$$

By transforming the equation, we obtain

$$\dot{\boldsymbol{\phi}} = \bar{B}^{\dagger}\bar{A}\dot{\boldsymbol{w}} + \mathcal{N}(\boldsymbol{q})\boldsymbol{\eta} \tag{4}$$

where $\bar{A}(\boldsymbol{q}) \in \mathbf{R}^{(n_b-m_b+3)\times 6}$ and $\bar{B}(\boldsymbol{q}) \in \mathbf{R}^{(n_b-m_b+3)\times(n-1)}$ are the matrices that the corresponding $i_1, \cdots, i_{m_b}$-th row vectors are eliminated from the original matrices A and B respectively, $\bar{B}^{\dagger}$ is the pseudo inverse matrix of $\bar{B}$, $\mathcal{N}(\boldsymbol{q}) \in \mathrm{Ker}(\bar{B})$ and $\boldsymbol{\eta} = [\boldsymbol{\eta}_h^T,\ \boldsymbol{\eta}_b^T]^T \in \mathbf{R}^m$, $\boldsymbol{\eta}_h \in \mathbf{R}^{m_h}$, $\boldsymbol{\eta}_b = [\eta_{b1}, \cdots, \eta_{bm_b}]^T \in \mathbf{R}^{m_b}$. $\mathcal{N}$ whose rows span the null space of $\bar{B}$ is the basis matrix of the internal motion which does not affect the motion of $\dot{\boldsymbol{w}}$, and $\boldsymbol{\eta}$ is the whole internal motion and $\boldsymbol{\eta}_b$ and $\boldsymbol{\eta}_h$ are the internal motions related to the base part and the head part respectively. The internal motion is caused by the kinematic redundancy of the robot. The kinematic redundancy "redundancy II" (the number of constraint equation is less than the number of input : $n_b - m_b + 3 < n - 1$) is defined in [3]. The internal motion of the snake robot is caused by increasing links of the head part and removing wheels of the base part, and we obtain $\mathcal{N}\boldsymbol{\eta} = \mathcal{N}_h\boldsymbol{\eta}_h + \mathcal{N}_b\boldsymbol{\eta}_b$.

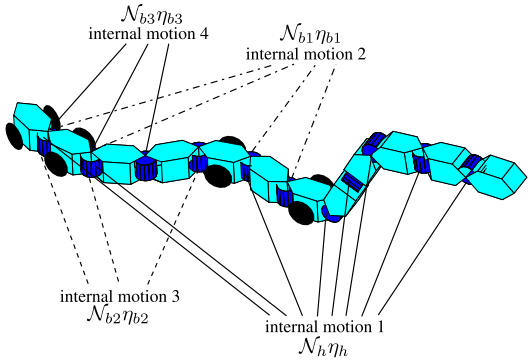

Fig. 2. The internal motion caused by removing wheels of the 12-link snake robot

A popular approach for control of a redundant manipulator is controlling internal dynamics related to the kinematic redundancy by using a basis matrix $\mathcal{N}$ of the internal motion [11]. In the case of applying this approach to the complicated nonlinear system such as snake robots, deriving the basis and obtaining its differential are hard. So we consider that the shape controllable point (SCP) is treated as the representation of the redundancy [3][4].

From the structure of $\bar{B}$, the basis matrix $\bar{\mathcal{N}}$ whose row vectors span the null space of $\bar{B}$ is expressed as

$$\bar{\mathcal{N}} = \begin{bmatrix} \bar{\boldsymbol{v}}_{1h} & & & & \cdots & & & \bar{\boldsymbol{v}}_{(n-1)h} \\ 0 & \cdots & 0 & \bar{v}_{(i_1-1)1} & & \cdots & & \bar{v}_{(n-1)1} \\ \vdots & & & & \ddots & & & \vdots \\ 0 & & \cdots & & 0 & \bar{v}_{(i_{m_b}-1)m_b} & \cdots & \bar{v}_{(n-1)m_b} \end{bmatrix}^T \tag{5}$$

where $\bar{\boldsymbol{v}}_{ih} \in \mathbf{R}^{m_h}$. By some operations of deleting and adding the column vectors of (5) we derive the basis matrix

$\mathcal{N}$ of the internal motion. It is expressed as

$$
\begin{aligned}
\mathcal{N} &= [\mathcal{N}_h \ \mid \ \mathcal{N}_b] \\
&= [\mathcal{N}_h \ \mid \ \mathcal{N}_{b1} \ \mathcal{N}_{b2} \ \cdots \ \mathcal{N}_{bm_b}] \\
&= \left[\begin{array}{c|cccc}
\boldsymbol{v}_{1h} & 0 & 0 & \cdots & 0 \\
\vdots & \vdots & & & \\
\boldsymbol{v}_{(i_1-2)h} & 0 & & & \\
\boldsymbol{0} & v_{(i_1-1)(m_h+1)} & \vdots & & \\
\boldsymbol{v}_{i_1 1} & v_{i_1(m_h+1)} & & & \\
\vdots & \vdots & & & \vdots \\
\boldsymbol{v}_{(i_2-2)h} & v_{(i_2-2)(m_h+1)} & 0 & & \\
\boldsymbol{0} & 0 & v_{(i_2-1)(m_h+2)} & & \\
\boldsymbol{v}_{i_2 h} & v_{i_2(m_h+1)} & v_{i_2(m_h+2)} & & \\
\vdots & \vdots & \vdots & \ddots & \\
\boldsymbol{v}_{(i_{m_b}-2)h} & v_{(i_{m_b}-2)(m_h+1)} & v_{(i_{m_b}-2)(m_h+2)} & & 0 \\
\boldsymbol{0} & 0 & 0 & & v_{(i_{m_b}-1)m} \\
\boldsymbol{v}_{i_{m_b} h} & v_{i_{m_b}(m_h+1)} & v_{i_{m_b}(m_h+2)} & & v_{i_{m_b} m} \\
\vdots & \vdots & \vdots & & \vdots \\
\boldsymbol{v}_{(n-1)h} & v_{(n-1)(m_h+1)} & v_{(n-1)(m_h+2)} & \cdots & v_{(n-1)m}
\end{array}\right]
\end{aligned}
\tag{6}
$$

where $\boldsymbol{v}_{ih} \in \mathbf{R}^{1\times m_h} (i = 1, \cdots, n-1)$.

From (6), we find that $\mathcal{N}_{bj}\eta_{bj}$ $(j = 1, \cdots, m_b)$ affects $\dot{\phi}_{i_j-1}$ and $\dot{\phi}_k$ $(k > i_j - 1, \quad k \neq i_j - 1, \cdots, i_{m_b} - 1)$. $\dot{\phi}_{i_j-1}$ is the joint velocity corresponding to the j-th unwheeled link and $\dot{\phi}_k$ is corresponding to the wheeled link which is posterior to j-th wheelless link. Note that $\mathcal{N}_b\boldsymbol{\eta}_b$ does not affect joints velocities which are anterior to the joint velocity $\dot{\phi}_{i_1}$ corresponding to the first wheelless link. The joint angles ϕ_{i_j-1} of the wheelless link of the base part is introduced into the controlled variables $\boldsymbol{w}$ as the representation of the kinematic redundancy of the base part [3]. In this paper, we call $\tilde{\boldsymbol{\phi}}_b = [\tilde{\phi}_{b1}, \cdots, \tilde{\phi}_{bm_b}]^T = [\phi_{i_1-1}, \cdots, \phi_{i_{m_b}-1}]^T \in \mathbf{R}^{m_b}$ "base shape controllable point (B-SCP)". These representations seem to be appropriate because B-SCPs have one-to-one relation with each internal motion $\boldsymbol{\eta}_b$ of the base part and the number of B-SCPs is equal to the degree of $\boldsymbol{\eta}_b$.

On the other hand, $\mathcal{N}_h\boldsymbol{\eta}_h$ caused by redundant links of the head part affects velocities of all joint except B-SCPs $\tilde{\boldsymbol{\phi}}_b$. Since the degree of the internal motion $\boldsymbol{\eta}_h$ of the head part is m_h, we introduce the m_h joint angles of the head part $\tilde{\boldsymbol{\phi}}_h = [\tilde{\phi}_{h1}, \cdots, \tilde{\phi}_{hm_h}]^T \in \mathbf{R}^{m_h}$ into the variables to be controlled $\boldsymbol{w}$ as the representation of the kinematic redundancy of the head part. We call $\tilde{\boldsymbol{\phi}}_h$ "head shape controllable point (H-SCP)".

For example, Fig. 2 shows the internal motion of a 12 link snake robot where $n_h = 5$, $n_b = 7$, and wheels of the 7-th, 9-th and 10-th link are removed. In this case, the internal motion is $\boldsymbol{\eta} = [\eta_h, \eta_{b1}, \eta_{b2}, \eta_{b3}]^T \in \mathbf{R}^4$, $m_b = 3$, $m_h = 1$, and $\mathcal{N}$ is described as

$$
\begin{aligned}
\mathcal{N} &= [\mathcal{N}_h \ \mid \ \mathcal{N}_b] = [\mathcal{N}_h \mid \mathcal{N}_{b1} \ \mathcal{N}_{b2} \ \mathcal{N}_{b3}] \\
&= \left[\begin{array}{c|ccc}
v_{1h} & 0 & 0 & 0 \\
v_{2h} & & & \\
 & \vdots & \vdots & \vdots \\
v_{3h} & & & \\
v_{4h} & & & \\
v_{5h} & 0 & 0 & 0 \\
0 & v_{6b_1} & 0 & 0 \\
v_{7h} & v_{7b_1} & 0 & 0 \\
0 & 0 & v_{8b_2} & 0 \\
0 & 0 & 0 & v_{9b_3} \\
v_{10h} & v_{10b_1} & v_{10b_2} & v_{10b_3} \\
v_{11h} & v_{11b_1} & v_{11b_2} & v_{11b_3}
\end{array}\right].
\end{aligned}
$$

Therefore, the B-SCPs are $\tilde{\boldsymbol{\phi}}_b = [\phi_6, \phi_8, \phi_9]^T$, and the H-SCP is one of the joint angles of the head part.

We set all SCPs as $\tilde{\boldsymbol{\phi}} = [\tilde{\boldsymbol{\phi}}_h^T, \ \tilde{\boldsymbol{\phi}}_b^T]^T \in \mathbf{R}^m$, the vector excepts $\bar{\boldsymbol{\theta}}$ from $\boldsymbol{\phi}$ as $\bar{\boldsymbol{\theta}} \in \mathbf{R}^{n-m-1}$, and the state variables to be controlled as $\tilde{\boldsymbol{w}} = [\boldsymbol{w}^T, \tilde{\boldsymbol{\phi}}^T]^T$. The kinematic equation (3) is rewritten as

$$
\tilde{A}(\boldsymbol{q})\dot{\tilde{\boldsymbol{w}}} = \tilde{B}(\boldsymbol{q})\dot{\bar{\boldsymbol{\theta}}} \tag{7}
$$

By multiplying $\tilde{B}^{-1}$ from the left hand side to above equation, we obtain

$$
\dot{\bar{\boldsymbol{\theta}}} = \bar{F}\dot{\tilde{\boldsymbol{w}}} = \bar{F}_1\dot{\boldsymbol{w}} + \bar{F}_2\dot{\tilde{\boldsymbol{\phi}}}_h + \bar{F}_3\dot{\tilde{\boldsymbol{\phi}}}_b \tag{8}
$$

where $\bar{F} = \tilde{B}^{-1}\tilde{A} = [\bar{F}_1 \quad \bar{F}_2 \quad \bar{F}_3] \in \mathbf{R}^{(n-m-1)\times(6+m)}$. We set that the joint angles of the head part except H-SCP are $\bar{\boldsymbol{\theta}}_h \in \mathbf{R}^{n_h-m_h}$, the joint angles of the base part except B-SCP are $\bar{\boldsymbol{\theta}}_b \in \mathbf{R}^{n_b-m_b-1}$, and

$$
\dot{\bar{\boldsymbol{\theta}}} = [\dot{\bar{\boldsymbol{\theta}}}_h^T \quad \dot{\bar{\boldsymbol{\theta}}}_b^T]^T \tag{9}
$$

$$
= \left[\begin{array}{c} \bar{F}_{1h} \\ \bar{F}_{1b} \end{array}\right]\dot{\boldsymbol{w}} + \left[\begin{array}{c} \bar{F}_{2h} \\ \bar{F}_{2b} \end{array}\right]\dot{\tilde{\boldsymbol{\phi}}}_h + \left[\begin{array}{c} \boldsymbol{0} \\ \bar{F}_{3b} \end{array}\right]\dot{\tilde{\boldsymbol{\phi}}}_b \tag{10}
$$

where $\bar{F}_{1h} \in \mathbf{R}^{(n_h-m_h)\times 6}$, $\bar{F}_{1b} \in \mathbf{R}^{(n_b-m_b-1)\times 6}$, $\bar{F}_{2h} \in \mathbf{R}^{(n_h-m_h)\times m_h}$, $\bar{F}_{2b} \in \mathbf{R}^{(n_b-m_b-1)\times m_h}$, and $\bar{F}_{3b} = [\bar{F}_{3b1}, \cdots, \bar{F}_{3bm_b}]^T \in \mathbf{R}^{(n_b-m_b-1)\times m_b}$.

In this case, we provide following conditions.

[Condition 1] : The tail link is wheeled.
[Condition 2] : The direction of the rotational axes of all joints of the head part are not same.
[Condition 3] : H-SCPs are selected so that the direction of the rotational axes of all joints of the head part except H-SCPs are not same.
[Condition 4] : $1 \leq m < n - 7$.
[Condition 5] : $n_h \geq 4$.

Condition 1-3 are necessary condition for the full rankness of the matrix $\tilde{B}$, Condition 4 means that "the dimension of the state vector to be controlled $6 + m$ is less than the dimension of the input vector $n - 1 : 6 + m < n - 1$" and ensures that the kinematic redundancy of the system : $m > 1$. Condition 5 is needed in order to accomplish an arbitrary position and attitude of the snake head.

By considering the velocity constraint (8), we obtain the dynamic equation of the 3D snake robot as follows.

$$
\tilde{M}(\boldsymbol{q})\ddot{\tilde{\boldsymbol{w}}} + \tilde{h}(\boldsymbol{q}, \dot{\boldsymbol{q}}) = \tilde{E}\boldsymbol{\tau} \tag{11}
$$

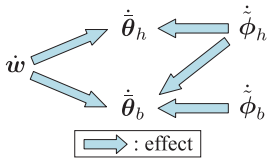

Fig. 3. The relationship among $\dot{\boldsymbol{q}}$ of a 3D snake robot

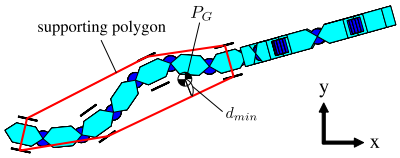

Fig. 4. The supporting polygon of a snake robot

III. CONTROLLER DESIGN FOR MAIN-OBJECTIVE

By using feedback linearization, let us define the control input $\boldsymbol{\tau}$ as

$$\boldsymbol{\tau} = \tilde{E}^{\dagger}\{\tilde{M}(\ddot{\tilde{\boldsymbol{w}}}_d - K_v\dot{\boldsymbol{e}} - K_p\boldsymbol{e}) + \tilde{h}\} + \boldsymbol{\tau}_{ker} \quad (12)$$

where $\tilde{E}^{\dagger}$ is a pseudo inverse matrix of $\tilde{E}$, $\boldsymbol{e} = \tilde{\boldsymbol{w}} - \tilde{\boldsymbol{w}}_d$, $\boldsymbol{\tau}_{ker}$ is an arbitrary vector which satisfies $\boldsymbol{\tau}_{ker} \in \mathrm{Ker}(\tilde{E})$. By selecting $K_v, K_p > 0$, $\tilde{\boldsymbol{w}}$ converges to the desired vector $\tilde{\boldsymbol{w}}_d$. $\boldsymbol{\tau}_{ker}$ is the term caused by the dynamical redundancy defined as "redundancy I" (the number of the state vector to be controlled $6+m$ is less than the number of the input vector $n-1$) in [3]. The kinematic redundancy is represented as the SCPs $\tilde{\boldsymbol{\phi}}$ which are included in $\tilde{\boldsymbol{w}}$ and we can use the kinematic redundancy by designing the desired value $\tilde{\boldsymbol{\phi}}_d$, appropriately.

IV. CONTROLLER DESIGN FOR SUB-OBJECTIVE

A. Desired value

We consider the increase of cost functions as sub-tasks. We proposed the control strategy that can ensure the convergence of the velocity of the SCPs to their desired values so as to accomplish the increase/decrease of one cost function $V(\boldsymbol{q})$ by using whole kinematic redundancy [4]. However, if the degree of the kinematic redundancy is multiple, we may be able to achieve several sub-tasks without trade-off of each sub-task.

From section II, the relationship between $\dot{\boldsymbol{q}}$ is shown as Fig. 3. Note that the velocity of the H-SCP $\dot{\tilde{\boldsymbol{\phi}}}_h$ affect $\dot{\tilde{\boldsymbol{\theta}}} = [\dot{\tilde{\boldsymbol{\theta}}}_h^T, \dot{\tilde{\boldsymbol{\theta}}}_b^T]^T$ and the velocity of the B-SCP $\dot{\tilde{\boldsymbol{\phi}}}_b$ does NOT affect $\dot{\tilde{\boldsymbol{\theta}}}_h$. Therefore, the sub-task of the H-SCP can be accomplished independently from the base part by setting the cost function $V_h(\boldsymbol{w}, \tilde{\boldsymbol{\phi}}_h, \tilde{\boldsymbol{\theta}}_h)$, which does not depend on joint angles of the base part. Let us define the desired values of the H-SCP $\dot{\tilde{\boldsymbol{\phi}}}_{hd}$ as

$$\dot{\tilde{\boldsymbol{\phi}}}_{hd} = a_h \left(\frac{\partial V_h}{\partial \tilde{\boldsymbol{\phi}}_h} + \frac{\partial V_h}{\partial \tilde{\boldsymbol{\theta}}_h} \bar{F}_{2h} \right)^T \quad (13)$$

where $a_h > 0$ is an appropriate gain coefficient. In the case that the H-SCP converges to their desired values, by considering (10), the time derivative of the cost function $V_h(\boldsymbol{w}, \tilde{\boldsymbol{\phi}}_h, \tilde{\boldsymbol{\theta}}_h)$ is approximately expressed as

$$\begin{aligned} \dot{V}_h &= \frac{\partial V_h}{\partial \boldsymbol{w}}\dot{\boldsymbol{w}} + \frac{\partial V_h}{\partial \tilde{\boldsymbol{\phi}}_h}\dot{\tilde{\boldsymbol{\phi}}}_h + \frac{\partial V_h}{\partial \tilde{\boldsymbol{\theta}}_h}\dot{\tilde{\boldsymbol{\theta}}}_h \\ &\simeq \left(\frac{\partial V_h}{\partial \boldsymbol{w}} + \frac{\partial V_h}{\partial \tilde{\boldsymbol{\theta}}_h}\bar{F}_{1h} \right) \dot{\boldsymbol{w}}_d \\ &\quad + a_h \left(\frac{\partial V_h}{\partial \tilde{\boldsymbol{\phi}}_h} + \frac{\partial V_h}{\partial \tilde{\boldsymbol{\theta}}_h}\bar{F}_{2h} \right) \left(\frac{\partial V_h}{\partial \tilde{\boldsymbol{\phi}}_h} + \frac{\partial V_h}{\partial \tilde{\boldsymbol{\theta}}_h}\bar{F}_{2h} \right)^T. \end{aligned} \quad (14)$$

As the first term of the right hand side of (14) does not depend on $\dot{\tilde{\boldsymbol{\phi}}}_h$ and the second term of the right hand side is positive definite, then controlling the H-SCP $\dot{\tilde{\boldsymbol{\phi}}}_h$ so as to converge to the desired values $\dot{\tilde{\boldsymbol{\phi}}}_{hd}$ makes the cost function V_h increasing.

Next, we consider the base part. we set the cost function $V_b(\boldsymbol{q})$ which should be increased by using the B-SCP $\tilde{\boldsymbol{\phi}}_b$ and let us define the desired velocity of the B-SCP $\dot{\tilde{\boldsymbol{\phi}}}_{bd}$ as

$$\dot{\tilde{\boldsymbol{\phi}}}_{bd} = a_b \left(\frac{\partial V_b}{\partial \tilde{\boldsymbol{\phi}}_b} + \frac{\partial V_b}{\partial \tilde{\boldsymbol{\theta}}_b} \bar{F}_{3b} \right)^T \quad (15)$$

where $a_b > 0$ is a gain coefficient. In the case that the B-SCPs converge to their desired values, the time derivative of the cost function $V_b(\boldsymbol{q})$ is approximately expressed as

$$\begin{aligned} \dot{V}_b &= \frac{\partial V_b}{\partial \boldsymbol{w}}\dot{\boldsymbol{w}} + \frac{\partial V_b}{\partial \tilde{\boldsymbol{\phi}}_h}\dot{\tilde{\boldsymbol{\phi}}}_h + \frac{\partial V_b}{\partial \tilde{\boldsymbol{\phi}}_b}\dot{\tilde{\boldsymbol{\phi}}}_b + \frac{\partial V_b}{\partial \tilde{\boldsymbol{\theta}}}\dot{\tilde{\boldsymbol{\theta}}} \\ &\simeq \left(\frac{\partial V_b}{\partial \boldsymbol{w}} + \frac{\partial V_b}{\partial \tilde{\boldsymbol{\theta}}}\bar{F}_1 \right) \dot{\boldsymbol{w}}_d + \left(\frac{\partial V_b}{\partial \tilde{\boldsymbol{\phi}}_h} + \frac{\partial V_b}{\partial \tilde{\boldsymbol{\theta}}}\bar{F}_2 \right) \dot{\tilde{\boldsymbol{\phi}}}_{hd} \\ &\quad + a_b \left(\frac{\partial V_b}{\partial \tilde{\boldsymbol{\phi}}_b} + \frac{\partial V_b}{\partial \tilde{\boldsymbol{\theta}}_b}\bar{F}_{3b} \right) \left(\frac{\partial V_b}{\partial \tilde{\boldsymbol{\phi}}_b} + \frac{\partial V_b}{\partial \tilde{\boldsymbol{\theta}}_b}\bar{F}_{3b} \right)^T. \end{aligned} \quad (16)$$

The first and second term in (16) do not depend on $\dot{\tilde{\boldsymbol{\phi}}}_b$, and the third term contributes the increase of V_b since it is positive definite. The second term in (16) is the effect of the H-SCP and the sub-task of the B-SCP is interfered by the H-SCP. However, this problem can be solved by adjusting a_b appropriately.

Consequently, by controlling SCPs as above discussion, the 3D snake robot can accomplish two sub-tasks which are the increase of V_h and V_b simultaneously.

B. Cost function

As the head part is used for the manipulation task mainly, the manipulability is important. So the increase of the manipulability of the kinematic model (7) is regarded as a sub-task of the head part. We set the cost function $V_h(\boldsymbol{w}, \tilde{\boldsymbol{\phi}}_h, \tilde{\boldsymbol{\theta}}_h)$ of the head part as

$$V_h(\boldsymbol{w}, \tilde{\boldsymbol{\phi}}_h, \tilde{\boldsymbol{\theta}}_h) = \det(\tilde{B}). \quad (17)$$

It is necessary for the snake robot to avoid the singular configuration where all passive wheels are parallel or an arc shape because the input torque diverges if the snake robot converges to the singular configuration. Thus, we regard the singularity avoidance as one sub-task of the base part. When $\tilde{E}$ in (11) is not full rank, the robot is the singular configuration. Additionally, the 3D snake robot has possibility of falling down. As shown in Fig. 4, the snake

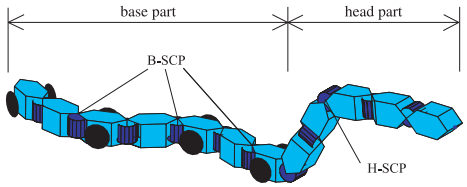

Fig. 5. The simulation model of a 3D snake robot

TABLE I

INITIAL CONFIGURATION AND DESIRED TRAJECTORY FOR SIMULATION

$\boldsymbol{w}(0)$	$[-0.2,\ -0.1,\ 0.44,\ 0,\ -1,\ \frac{\pi}{4}]^T$
$\boldsymbol{\phi}(0)$	$[-0.11, 0, 0, 0, 1.1, \frac{-\pi}{9}, \frac{\pi}{6}, \frac{\pi}{6}, \frac{-\pi}{9}, \frac{-\pi}{6}, \frac{-\pi}{10}]^T$
$\boldsymbol{w}_d$	$[0.2t, 0, 0.2, \frac{\pi}{6}, \frac{\pi}{6}, 0]^T$
K_v	$\mathrm{diag}(3, 3, 3, 2, 2, 2, 1, 1, 1, 1)$
K_p	$\mathrm{diag}(2, 2, 2, 1, 1, 1, 0, 0, 0, 0)$

robot is statically stable when the projective point P_G of the center of mass of the robot on the environment is contained within the supporting polygon of grounded wheels. We set the cost function $V_b(\boldsymbol{q})$ of the base part corresponding to $\tilde{\boldsymbol{\phi}}_b$ as

$$\begin{aligned} V_b(\boldsymbol{q}) &= a' V_{b1} + b' V_{b2} \\ &= a' \det(\tilde{E}\tilde{E}^T) + b' d_{min} \end{aligned} \tag{18}$$

where a', b' are nonnegative constants and d_{min} is the distance from P_G to the supporting polygon. The robot can avoid the singular configuration and reduce the risk of the fall by increasing the value of the above cost function.

V. SIMULATIONS

To demonstrate the effectiveness of the proposed control law simulations have been carried out. In this simulation we consider a 12-link snake robot where $n_h = 5$, $n_b = 7$, $m_h = 1$, $m_b = 3$, $l = 0.05$[m] and $l_w = 0.05$[m]. As shown in Fig. 5, the first, third and fifth links have pitch joints, other links have yaw joints, the seventh, ninth and eleventh links are unwheeled. We set that the H-SCP $\tilde{\phi}_h = \phi_3$, the B-SCP $\tilde{\boldsymbol{\phi}}_b = [\phi_6, \phi_8, \phi_{10}]^T$, $\tilde{\boldsymbol{w}} = [\boldsymbol{w}^T, \phi_3, \phi_6, \phi_8, \phi_{10}]^T$, and $\boldsymbol{\tau}_{ker} = \boldsymbol{0}$. Parameters of simulation are shown in Table I.

We consider following three control methods.

[case 1]: Kinematic redundancy is not used and the desired velocities of all SCPs are set as zero.
[case 2]: The sub-task corresponding to the H-SCP is set as the increase of static manipulability and the sub-task corresponding to the B-SCP is set as the singularity avoidance.
[case 3]: The sub-task corresponding to the H-SCP is set as the increase of the static manipulability and the sub-task corresponding to the B-SCP is set so as to avoid the singular configuration and the falls.

In [case 2] and [case 3], we set that the desired velocity of the H-SCP is (13), $a_h = 1.0 \times 10^5$, the desired velocity of the B-SCP is (15), and $a_b = 1$. In [case 2], $a' = 5 \times 10^{14}$ and $b' = 0$. In [case 3], $a' = 5 \times 10^{14}$ and $b' = 8.5$.

Fig. 6 shows the response of $\boldsymbol{w}$ in all cases, where a solid line represents the response of $\boldsymbol{w}$ and a broken line

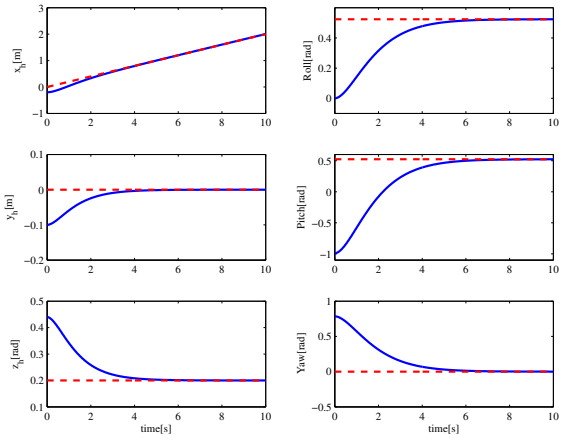

Fig. 6. Time responses of $\boldsymbol{w}$

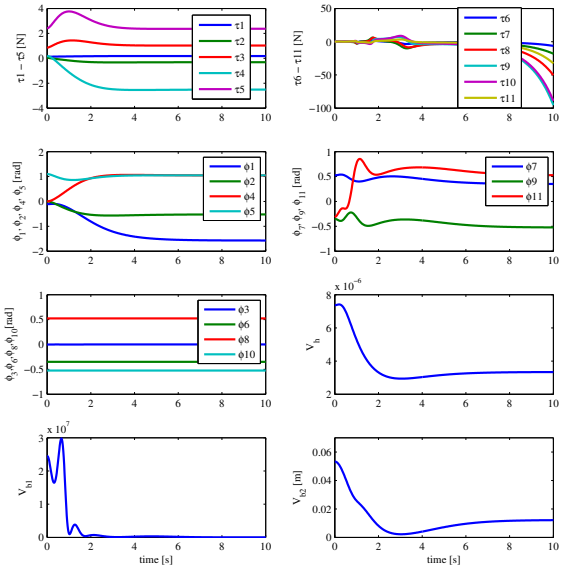

Fig. 7. Time responses of case 1

represents the desired trajectory. We find that the snake robot accomplishes the main task of the trajectory tracking of the snake head. Fig. 7-9 show the response of $\boldsymbol{\tau}$, $\tilde{\boldsymbol{\theta}}$, $\tilde{\boldsymbol{\phi}}$, the cost functions $V_h = \det(\tilde{B})$, $V_{b1} = \det(\tilde{E}\tilde{E}^T)$ and $V_{b2} = d_{min}$ of each case. Fig. 10 shows the motion of the snake robot in [case 3].

From Fig. 7, we find that V_{b1} converges to zero and the input torque of the base part diverges. This is because the singularity avoidance is not considered in this case.

In [case 2], we find that the value of V_h is larger than that of [case 1] and the robot accomplishes the avoidance of the singular configuration by increasing V_{b1} from Fig. 8.

In [case 3], from Fig. 9 we find that the singularity avoidance are accomplished as well as [case 2], and the minimum value of V_{b2} is 2.1×10^{-2}[m] which is larger than

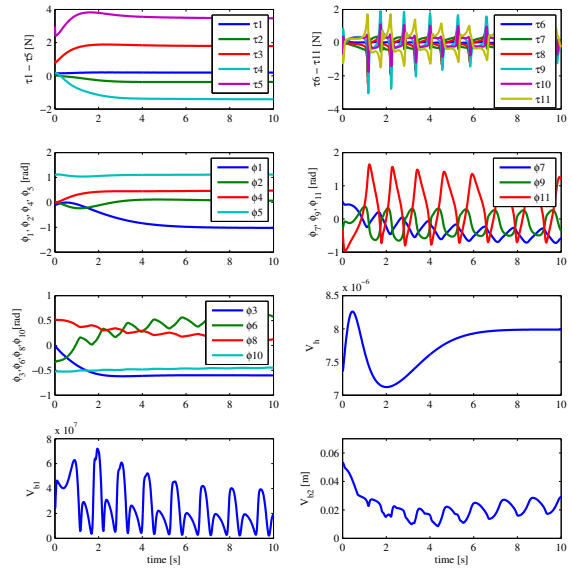

Fig. 8. Time responses of case 2

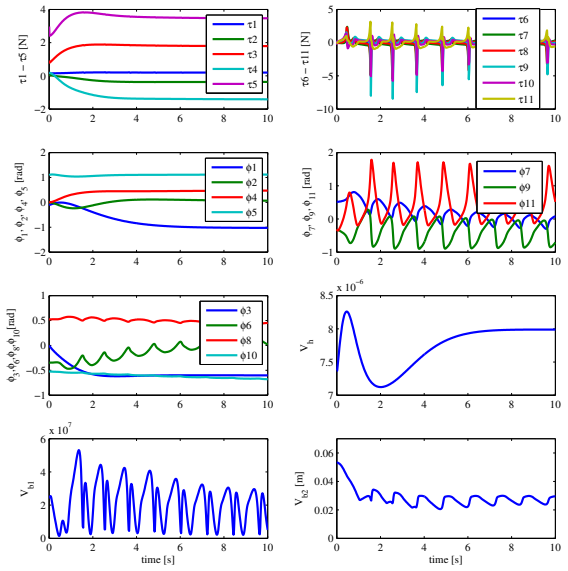

Fig. 9. Time responses of case 3

that of [case 2] 8.5×10^{-3}[m]. So, the reducing the risk of the falls is accomplished by increasing V_{b2}. Moreover, we can confirm that the increase of V_h is accomplished independently of the base part since the time response of V_h is exactly the same in [case 2] and [case 3]. However, the input torque of the base part in [case 3] is larger than that of [case 2] because there is trade-off relation between V_{b1} and V_{b2} as shown (18).

From these simulation results we find that the trajectory tracking as the main-task and several sub-tasks are accomplished by the proposed control strategy.

VI. CONCLUSION

We have considered the control of the redundant 3D snake robots based on the dynamic model. We analyzed features of the internal motion caused by the kinematic redundancy and represented the kinematic redundancy as shape controllable points for the dynamic model of the 3D snake robot. By utilizing kinematic redundancy and its features, we proposed the controller which accomplishes the trajectory tracking of the snake robot head and several sub-tasks. Simulation results ensure the effectiveness of the proposed control strategy. Future works are experimental demonstrations, considering the motion control on a nonplanar terrain, and so on.

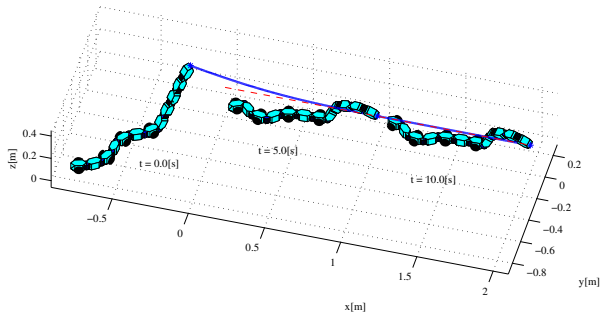

Fig. 10. The motion of the snake robot in case 3

REFERENCES

[1] S. Hirose, *Biologically Inspired Robots (Snake-like Locomotor and Manipulator)*, Oxford University Press, 1993.

[2] P. Prautsch, T. Mita and T. Iwasaki, "Analysis and Control of a Gait of Snake Robot", *Trans. of IEEJ*, Vol.120-D, pp.372-381, 2000.

[3] F. Matsuno and K. Mogi, "Redundancy Controllable System and Control of Snake Robot with Redundancy based on Kinematic Model", *Proc. IEEE Conf. on Decision and Control*, pp. 4791-4796, 2000.

[4] F. Matsuno and H. Sato, "Trajectory tracking control of snake robot based on dynamic model", *Proc. IEEE Int. Conf. on Robotics and Automation*, pp.3040-3046, 2005.

[5] S. Ma, Y. Ohmameuda and K. Inoue, "Dynamic Analysis of 3-dimensional Snake Robots," *Proc. IEEE/RSJ Int. Conf. on Intelligent Robots and Systems*, pp.767-772, 2004.

[6] H. Date and Y. Takita, "Control of 3D snake-like locomotive mechanism based on continuum modeling," *Proc. ASME2005 Int. Design Engineering Technical Conf.*, No. DETC2005-85130, 2005.

[7] M. Yamakita, M. Hashimoto and T. Yamada, "Control of Locomotion and Head Configuration for 3D Snake Robot", Journal of the Robotics Society of Japan, Vol.22, No.1, pp.61-67, 2004 (in Japanese).

[8] F. Matsuno and K. Suenaga, "Control of Redundant 3D Snake Robot based on Kinematic Model," *Proc IEEE Int. Conf. on Robotics and Automation*, pp.2061-2066, 2003.

[9] Y. Yamamoto and X. Yun, "Effect of the Dynamic Interaction on Coordinated Control of Mobile Manipulators, " *IEEE Trans. on Robotics and Automation*, Vol. 12, No. 5, 1996.

[10] M. Tanaka and F. Matsuno, "Cooperative Control of Two Snake Robots", *Proc. IEEE Int. Conf. on Robotics and Automation*, pp.400-405, 2006.

[11] R. Murray, Z. Li and S. Sastry, *A Mathematical Introduction to Robotic Manipulation*, CRC Press, 1994.